Lectures on Mathematics in the Life Sciences
Volume 18, 1986

Dynamics of stomate fields in leaves

Richard H. Rand and J. L. Ellenson

ABSTRACT. Experimental evidence is presented to show that nonsynchronous behavior of stomata at different positions on the same leaf occurs in real leaves. For example, if the condition of the leaf is suddenly changed, such as by quickly altering its water status or its exposure to light, the transient process of stomatal opening or closing may occur gradually, in a spatially organized fashion, i.e., in a wave.

We review the recent literature on mathematical models of stomatal dynamics and generalize previous work by presenting a new model which describes the effects of coupling on the dynamics of a stomate field. The coupling mechanism is the diffusion of water potential.

The model takes the form of a piecewise linear system consisting of a partial differential equation coupled to two ordinary differential equations.

It is shown that the whole leaf model can exhibit steady state oscillations even though the individual stomate model cannot.

0075-8523/86 $1.00 + $.25 per page

INTRODUCTION

This work concerns a mathematical model of the flow of water in leaves. We shall begin by introducing the reader to the biological problem (see Rand [1], Nobel [2]).

Leaves are the site of photosynthesis, the process by which the energy of the sun is harnessed to provide food. This process requires sunlight, carbon dioxide, and water, and produces glucose (a simple sugar) and oxygen.

The carbon dioxide enters the leaf by diffusion through small pores called stomata (Fig. 1). The thinness of leaves is accounted for by the well-known effectiveness of diffusion over small distances. Thus the leaf breathes without the use of a lung-like mass transport system.

A drawback of this gaseous diffusion mechanism, however, is the loss of water by evaporation through these same stomatal pores. Water loss is generally thought to be undesirable, especially in times of drought.

The situation is aided, however, by the fact that the stomatal pores are not fixed in size, but rather are formed by the sides of two specialized leaf cells called guard cells (Fig. 2). Due to its elastic cell walls, the shape of a guard cell may be changed by a change in its internal hydrodynamic pressure, thus altering the pore size. This hydrodynamic pressure, in turn, can be influenced by the leaf illumination (through light-sensitive chemical reactions), by the availability of ambient carbon dioxide, and by the availability of water in the leaf. Thus stomata can

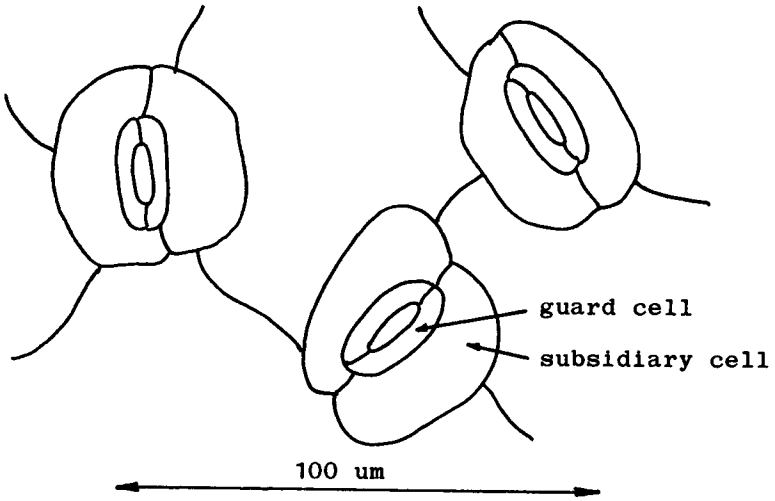

Fig. 1. View of the leaf surface showing stomatal pores.

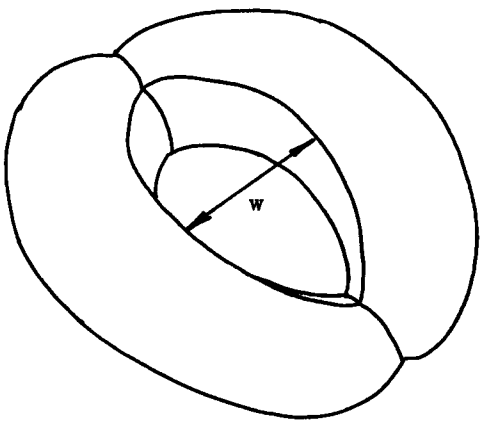

Fig. 2. The stomatal pore is formed by the sides of a pair of guard cells. The dimension w represents the pore width.

act like valves to limit the loss of water by evaporation. For example, stomata are generally closed at night when the absence of sunlight prevents photosynthesis.

The individual stomatal unit consists of a pair of guard cells together with neighboring subsidiary cells. Together with water which is available from the rest of the leaf, these cells form a dynamical system. It is capable of oscillating as well as of attaining steady state equilibrium.

Water which is lost through the stomatal pores is replaced by a flow through the plant called the transpiration stream. This flow originates in the roots and travels through the body of the plant to the leaves through a vascular tissue called the xylem. Once inside the leaf the water flows along the familiar system of branching xylem vessels to the xylem termini, and then continues through the cell walls to those cells near the stomatal pore where evaporation occurs. Flow through the interiors of cells (the symplasm) is thought to be negligible compared with the more efficient pathway through the matrix of cell walls (the apoplasm).

In this work we shall be interested in the dynamics of the flow of water through the leaf, assuming that each of the stomatal pores is an independent dynamical unit, able to open or close in response to the local availability of water. The latter may be expressed quantitatively by using a concept invented by plant physiologists called water potential. Water potential is a field quantity, comparable to temperature in problems of heat conduction. The flow of water is proportional to the negative gradient of the water

potential, just as heat flux is proportional to the negative gradient of the temperature.

Thus the water potential field in the leaf influences the state of the stomata. On the other hand, the extent of stomatal opening effects the diffusion of water potential by providing a sink through which water escapes from the leaf. Our goal in this paper is to propose a model for this interaction.

LITERATURE REVIEW

In this section we briefly review previous mathematical models of related problems in leaf dynamics.

Cooke et al. [7] investigated the elastostatics of a stomatal guard cell by using a linear anisotropic thin-shell model and finite element analysis. This work showed that the size of the stomatal pore was influenced independently by the pressure u in the guard cell and by the pressure v in the subsidiary cell. An increase in u tended to open the pore, while an increase in v tended to close the pore. More specifically, if w represents the width of the pore, the following relationship was obtained:

$$w = (c_1 u - c_2 v)\, H(c_1 u - c_2 v) \tag{1}$$

where H(.) = the Heaviside step function
w = width of pore
u = guard cell pressure
v = subsidiary cell pressure

c_1, c_2 = positive proportionality constants

which depend upon material properties and guard cell geometry.

That is, w is a ramp function of a linear combination of u and v. The source of the slope discontinuity in (1) is found in the geometry of the pair of guard cells. Since w is the distance between the boundaries of two neighboring cell walls, it can never become negative since the walls cannot pass through each other. Geometrically eq.(1) divides the u-v plane into two regions, see Fig. 3. In one of these regions, w is identically zero for all values of u and v, while in the other, w is proportional to the distance from the line $c_1 u = c_2 v$.

Eq.(1) was the basis for two dynamical studies of the stomatal apparatus (Delwiche & Cooke [3], Rand et al. [4]). By taking into account the flow of water between the guard cells, the subsidiary cells, the rest of the leaf and the air outside the leaf, Delwiche & Cooke [3] were able to derive a model which had the pressures u and v as time dependent state variables. The model took the form of a pair of nonlinear ordinary differential equations representing a flow on the u-v phase plane. Rand et al. [4] analyzed this model and showed that for a narrow range of parameters it supported the creation of limit cycles through Hopf and other bifurcations, although its more typical dynamics consisted of the global approach to stable equilibria. In particular this model accounts for experimental observations in which stomata are observed to temporarily close during the process of opening, Fig.4.

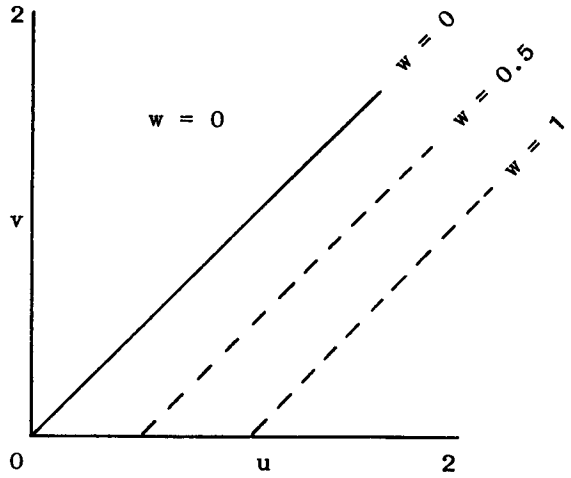

Fig. 3. The u-v plane is divided into two regions. In one region w=0 while in the other $w > 0$. The variables u and v represent the pressures in the guard and subsidiary cells, respectively.

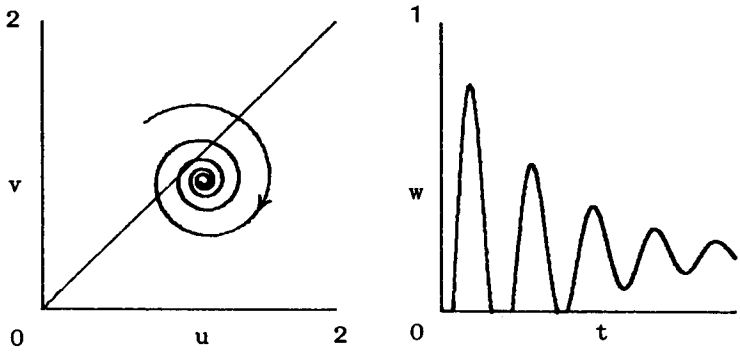

Fig. 4. Model based on a flow in the u-v phase plane predicts that a stomate can temporarily close during the process of opening.

These stomatal dynamics models motivated a study of a system of coupled stomatal units (Rand et al. [5]). This model omitted reference to the u-v phase plane, but rather modeled the individual stomatal unit as being either open, closed, or in an oscillatory state, depending upon the local water potential. When in the oscillatory state, an individual stomatal oscillator was represented by a single state variable, its phase. The water potential itself was assumed to satisfy a diffusion equation. A one dimensional array of such coupled units was shown to exhibit complicated dynamics and suggested the theoretical possibility of waves of stomatal opening passing across the leaf surface.

The model presented in this paper is seen as an extension of this previous work on coupled stomatal units. We will model the individual units by a flow on the phase plane, coupled by diffusion of water potential. Before discussing the model, however, we present a summary of some new experimental results. These observations provided the motivation for the current model. Needless to say, experimental results are essential for the design and evaluation of any such model.

EXPERIMENTAL RESULTS

The experimental procedures used in this work were based on the following phenomenology (see also Ellenson and Amundson [6]):

Plant leaves that have been illuminated by light emit a very low level of luminescence. This luminescence results when light-generated photosynthetic intermediates recombine in the dark to

regenerate the same electronically-excited state of chlorophyll that gives rise to fluorescence. This process is essentially photosynthesis in reverse, in that chemical energy is converted into light energy.

This luminescence, called delayed light emission (DLE), has been attributed to reactions that are involved with the oxygen-producing portion of the photosynthetic reaction pathway. DLE is totally dependent upon the integrity of the photosynthetic electron transport system. Because the electron pathways that are involved in the production of DLE are the same ones that are involved in photosynthesis, a disruption in photosynthetic activity invariably leads to a change in the amount of DLE that is emitted by a plant. Normally, inhibition of electron transport results in an increase in DLE, reflecting the inability of the plant to make use of the incident light energy.

In practice, because DLE has the same emission spectrum as chlorophyll fluorescence which is emitted when a light is directly shining on chlorophyll molecules, the only way to detect DLE is to observe the luminscence after the light has been extinguished. And, because the intensity of DLE rapidly diminishes following the extinction of the light, the best way to measure the luminescence is to rapidly flash a light source on a leaf sample and observe the luminescence emitted in the dark periods between flashes. By employing an image intensifier (a starlight scope), i.e., an electro-optical device that provides images of extremely low illumination subjects, it is possible to use DLE to monitor the temporal and spatial distribution of photosynthetic activity in intact plant leaves.

In this example, a single red kidney bean leaf has been contained within a two-compartmented chamber that enables the observer to regulate the atmospheric conditions surrounding the two bilateral halves of single leaf samples. This permits a single leaf to serve as both an experimental sample and a control sample. By analyzing the air stream entering and leaving the two chambers, one can investigate how photosynthetic processes, measured by the uptake of CO2 from the inlet air stream, are affected by various environmental perturbations. In addition, temporal and spatial changes in the rate of CO2 entry into the leaf can be observed as changes in DLE intensity. In this manner, both the gross overall changes in whole leaf physiology as well as localized changes in photosynthetic activity can be monitored.

In order to enhance changes in DLE caused by changes in gas exchange, gaseous SO2 was introduced into the upper chamber of the leaf cuvette in the experiments reported here. This enhancement is the result of a reversible inhibition of electron transport by SO2. Because of the gaseous nature of SO2, the reversible nature of the SO2 inhibition of electron transport, and the sensitivity of DLE to SO2, the introduction of SO2 into the inlet air stream serves to enhance the DLE emission in those areas of the leaf where CO2 (and SO2) can enter.

In practice, DLE is detected by rapidly flashing the plant leaf with bright white light and observing the leaf in the dark period between the flashes. In this work, a flash rate of 40 Hz was used, so that the DLE was observed between about 10 and 15 msec after each flash of light (which lasted approximately 10 msec.)

A record of the resulting leaf images was recorded on video tape. Fig. 5 shows a sample image. The lighter parts of the image correspond to those regions of the leaf in which photosynthesis is occurring and which therefore have open stomata. Examination of a sequence of such images reveals the lighter region to gradually spread out, and then to contract, and this behavior to occur repeatedly for several hours, with a period of about 30 minutes. These images correspond to a wave of stomatal opening and closing moving in the plane of the leaf, and may be associated with a transient dynamic accompanying the opening of the stomates when the lights were suddenly turned on.

DESCRIPTION OF THE MODEL

In describing the model we must state i) how to model the dynamics of the individual stomatal unit, and ii) how to model the coupling between neighboring stomatal units.

The individual stomatal units are modeled by a flow on the u-v phase plane, where, as before, u and v are the hydrodynamic pressures in the guard and subsidiary cells, respectively. We generalize the work of Delwiche and Cooke [3], and of Rand et al. [4], and propose a general flow of the form:

$$(2) \qquad u_t = f(u,v;z), \quad v_t = g(u,v;z)$$

in which $z = z(x,y,t)$ represents the water potential at the point (x,y) on the leaf. Here (x,y) tags the position of a particular stomatal unit. As in the work

Fig. 5. Sample image of DLE video recording of a single leaf. Lighter regions correspond to open stomata.

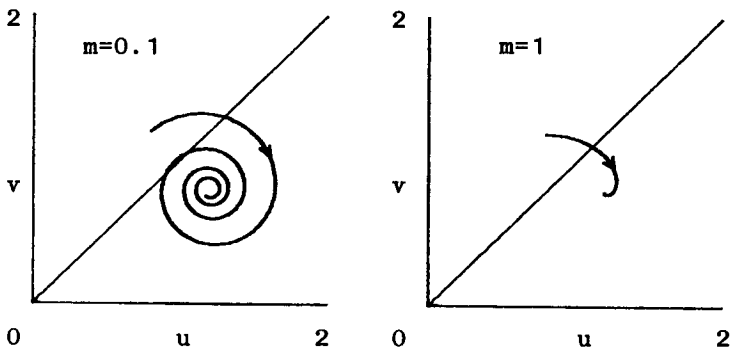

Fig. 6. Behavior of eqs.(5) for m=0.1 and m=1, with z=0.2. Each individual stomate is modeled as a damped linear oscillator and cannot exhibit steady state oscillations.

of Cooke et al. [7] we assume that the extent of stomatal opening w is a piecewise linear function of the pressures u,v:

$$w = (u-v)\, H(u-v) \tag{3}$$

where H(.) is the Heaviside step function.

The flow (2) is assumed to exhibit a stable equilibrium point in the u-v plane, the location of which depends on the parameter z. As z increases, physically representing a local increase in the availability of water, the location of the equilibrium point is assumed to move so as to tend to increase w, i.e., in a direction perpendicular to the line u = v.

In an effort to present a simpler (and thus easier to understand, although less realistic) model of the flow (2) than was previously considered in [3] and [4], we propose a linear flow of the form:

$$\begin{aligned} u_t &= a\,(u-F(z)) + b\,(v-G(z)) \\ v_t &= c\,(u-F(z)) + d\,(v-G(z)) \end{aligned} \tag{4}$$

where a,b,c,d are coefficients and (F(z),G(z)) is the location of the equilibrium. Since this flow is linear, it cannot exhibit a limit cycle. Although the model in [3] and [4] did exhibit limit cycles for a narrow range of parameters, these steady state oscillations must be viewed as exceptional in terms of the behavior of real plants. By choosing the parameters in (4) appropriately we can model more

typical leaf dynamics.

In particular, we choose a flow which for fixed z represents a damped oscillator, in agreement with many experimental observations of leaves. In terms of (4), this leads us to choose $a = d = -m$, $b = -c = 1$, $F(z) = z+1$, $G(z) = -z+1$, i.e.

$$u_t = -m\,(u-z-1) + (v+z-1)$$

(5)

$$v_t = -(u-z-1) - m\,(v+z-1)$$

Here the parameter m represents the extent of damping. Time has been effectively scaled so that the frequency of oscillation is unity. The system (5) has an equilibrium position at $u = 1+z$, $v = 1-z$, which lies along the line $u+v = 2$ in the u-v plane. For $z < 0$ this equilibrium corresponds to $w = 0$ (closed pore) since then $u < v$, cf. eq. (3). See Fig. 6 in which the behavior of the system (5) is displayed.

Next we must state how the individual stomatal units, modeled by eqs.(2)-(5), are coupled. We shall assume, after Rand et al. [5] that coupling is due to diffusion of water potential $z(x,y,t)$ through the leaf. The physical path through the leaf which we are modeling is the apoplasm, i.e., the xylem vessels and the cell wall pathways which form a connected matrix for the flow of water. In addition to the usual terms in the diffusion equation, there is a local sink due to water exiting the leaf in the case that the local stomatal pore is open (i.e., if $w > 0$). These considerations lead us to propose the following

equation for the diffusion of water potential:

$$(6) \qquad z_t = D\,(z_{xx} + z_{yy}) - Q(w)$$

where D is a diffusion coefficient, and where the function Q(w) represents the loss of water due to evaporation through the open stomatal pore.

It is clear that Q(w) must be a monotone increasing function (since an increase in pore width w cannot decrease the flux through the pore.) In a previous study (Holcomb & Cooke [8], Cooke and Rand [9]) a realistic but complicated expression for Q(w) was obtained. In order to make the present model as simple as possible, we assume that Q(w) = k w, i.e. evaporative water loss is proportional to pore size. This gives the equation:

$$(7) \qquad z_t = D\,(z_{xx} + z_{yy}) - k\,w$$

In summary, the present model consists of eqs.(5) and (7), with the pore size w defined by (3). The state variables are the pressures u(x,y,t), v(x,y,t), and the water potential z(x,y,t). The parameters are m (the damping associated with an individual stomatal unit), D (the diffusion coefficient of water flow in the plane of the leaf) and k (the leakage coefficient measuring water loss through open pores.)

STABILITY OF THE EQUILIBRIUM STEADY STATE

We consider a one dimensional version of this model for which the variables u,v and z depend on x and t only. We assume boundary conditions of the form

$$z = z0 \quad , \; x = 0 \tag{8}$$

where z0 is the applied water potential at the petiole, x=0, and

$$z_x = 0 \; , \; x = 1 \tag{9}$$

representing no flux in the plane of the leaf at the leaf edge, x = 1. Here length has been effectively scaled so that the leaf has length unity.

If we assume that at steady state all pores remain open, i.e., w = u-v > 0 in eq.(3), then eq.(7) becomes

$$z_t = D\, z_{xx} - k\,(u - v) \tag{10}$$

Eqs.(5),(10) give the following steady state solution:

$$z_{ss} = z0 \;\cosh p(1-x) \,/\, \cosh p \tag{11}$$

$$u_{ss} = 1 + z_{ss} \tag{12}$$

$$v_{ss} = 1 - z_{ss} \tag{13}$$

where $p^2 = 2\ k\ /\ D$.

In order to investigate the stability of this steady state solution, we set

$$z(x,t) = z_{ss}(x) + Z(x,t) \tag{14}$$

$$u(x,t) = u_{ss}(x) + U(x,t) \tag{15}$$

$$v(x,t) = v_{ss}(x) + V(x,t) \tag{16}$$

The steady state solution will be said to be stable if all solutions U,V,Z are bounded as t goes to infinity, and unstable if an unbounded solution exists.

Substitution of (14)-(16) into eqs.(5),(8)-(10) gives the linear system

$$Z_t = D\ Z_{xx} - k\ (U - V) \tag{17}$$

$$U_t = -\ m\ (U - Z) + (V + Z) \tag{18}$$

$$V_t = -\ (U - Z) - m\ (V + Z) \tag{19}$$

subject to the boundary conditions

$$Z(0,t) = 0, \quad Z_x(1,t) = 0 \tag{20}$$

We seek a solution to (17)-(20) in the form

$$Z(x,t) = e^{rt} f(x) \tag{21}$$

$$U(x,t) = e^{rt} g(x) \tag{22}$$

$$V(x,t) = e^{rt} h(x) \tag{23}$$

After substituting (21)-(23) into (18)-(19), we obtain

$$g(x) = f(x)\,(m^2 + rm + 1 + r)/[(r + m)^2 + 1] \tag{24}$$

$$h(x) = -\,f(x)\,(m^2 + rm + 1 - r)/[(r + m)^2 + 1] \tag{25}$$

Substituting (21)-(25) into (17) gives

$$f'' + A f = 0, \tag{26}$$

where

$$A = -\,\frac{r^3 + 2m\,r^2 + (m^2 + 2km + 1)\,r + 2k(m^2+1)}{D\,[(r + m)^2 + 1]} \tag{27}$$

Using the boundary conditions (20), we solve (26) as

$$f(x) = \sin(n\pi x / 2), \quad n = 1,3,5,\ldots \tag{28}$$

where r is given by the condition

$$A = (n \pi / 2)^2 \tag{29}$$

where A is defined in eq.(27).

Eq.(29) represents a cubic on r:

$$r^3 + a\, r^2 + b\, r + c = 0 \tag{30}$$

where $a = d + 2m$

$$b = m^2 + 2\,(d + k)\, m + 1$$

$$c = (d + 2k)\,(m^2 + 1)$$

where $d = D\,(n \pi / 2)^2$

The coefficients a,b,c are positive for positive values of the parameters m,k and D. Thus Descartes' rule of signs shows that there exist no positive roots, and either 3 negative roots or 1 negative root and 2 complex conjugates. For an unstable solution we must therefore have a pair of complex conjugate roots with positive real part.

The transition to instability will occur when (30) has a pair of pure imaginary roots r = is, r = -is, and a negative root r = -q:

$$(31) \quad (r^2 + s^2)(r + q) = r^3 + q\,r^2 + s^2\,r + qs^2 = 0$$

Comparison of (31) with (30) shows that for a transition to instability we require

$$(32) \qquad a = q, \quad b = s^2, \quad c = qs^2, \qquad \text{or}$$

$$(33) \qquad a\,b = c$$

which may be written in the form

$$(34) \quad k = K = -\,m\,[(m+d)^2 + 1] \,/\, (m^2 + dm - 1)$$

For given m and d, the critical value of k, called K in eq.(34), divides the k-line into two parts, one corresponding to stable points, the other to unstable points.

For the special case in which k = 0, eq.(30) has the roots

$$(35) \quad r = -d, -m + i, -m - i, \qquad (k = 0),$$

and thus represents a stable steady state (11)-(13). This case may be considered to correspond to the situation in which all pores are closed at steady state, in which case there would be no leakage term in eq.(10).

Since the point k = 0 always lies in the stable region, there are two cases to be considered:

(i) $K > 0$. In this case, when $k > K > 0$, the cubic (30) admits roots with positive real parts and the steady state is unstable. When $0 < k < K$, the steady state is stable. See Fig.7a.
(ii) $K < 0$. Since k is necessarily positive, in this case we see that $k > 0 > K$, and no instability is possible. See Fig.7b.

In order to distinguish between cases (i) and (ii), we consider the sign of K in (34). Let us fix m and let d vary from 0+ to infinity. K changes sign when the denominator of (34) vanishes, i.e., when

$$d = (1/m) - m \tag{36}$$

Thus when $m > 1$, the value of d given by (36) is negative, and so $K < 0$ and we are always in case (ii), i.e. no instability is possible.

When $m < 1$, however, we can be in either case. If d lies in the interval I,

$$I: 0 < d < (1/m) - m \tag{37}$$

then $K > 0$ and instability is possible.

Now recall (cf. eq.(30)) that $d = D (n \pi/2)^2$ for $n = 1,3,5,\ldots$. Corresponding to each value of n is a value of K in (34). Assuming that we are in the case of $m < 1$, we must ask which n gives the smallest value of K ? (Cf. Fig. 7a.) If, for fixed m, K is monotone increasing for d in I, then the smallest K corresponds to the smallest d, i.e., $n = 1$.

We prove that K is monotone increasing for d in I by showing that the derivative of K with respect to d, call it K', is positive over this range. In fact

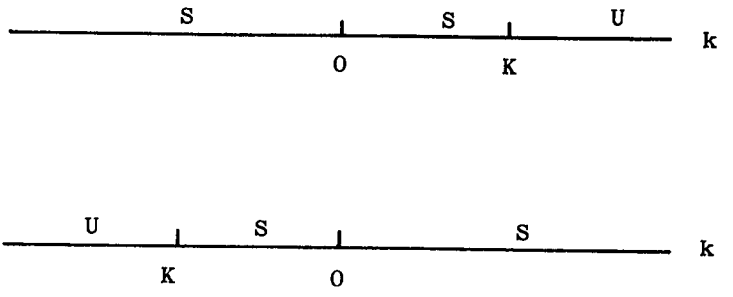

Fig. 7. Stability of the equilibrium steady state. S=stable, U=unstable.
a) When $K > 0$ (upper figure), both stable and unstable states are possible for $k > 0$.
b) When $K < 0$ (lower figure), no instability is possible for $k > 0$.

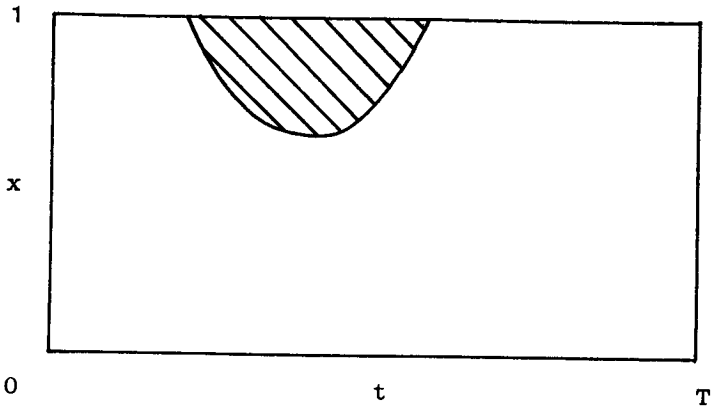

Fig. 8. The periodic steady state motion is associated with a curve in the x-t plane which separates open-pore (unshaded) regions from closed-pore (shaded) regions. T is the period of the motion.

$$(38) \qquad K' = \frac{m\,[\,-md^2 + 2(1-m^2)d + m(3-m^2)\,]}{(m^2 + dm - 1)^2}$$

At d=0, $K' > 0$ since $m < 1$. Thus we only have to show that K' has no zeros for d in I. Now $K' = 0$ when

$$(39) \qquad d = (1/m) - m \pm [(1/m)^2 + 1]^{1/2}$$

Do either of these roots lie in the interval I given by (37) ? Certainly the root corresponding to the + sign does not. Also, for $m < 1$, the square root term in (39) is larger than unity, while $(1/m) - m < 1$, and therefore the value of d corresponding to the - sign is negative and hence does not lie in I. Thus the zeros of K' do not lie in I and the smallest value of K occurs for n=1.

In conclusion, the steady state (11)-(13), which assumes that all pores are open, will be unstable if m and D are sufficiently small and if k is sufficiently large. Specifically, for instability we require that

$$(40) \qquad m < 1, \quad d < (1/m) - m,$$

and $$k > -m[(m+d)^2+1]/(m^2+dm-1)$$

where $d = D\,(\pi/2)^2$.

We also showed that the steady state $z = z0$ which assumes that all pores are closed (and which can be obtained from (11) by setting $k = 0$) is always stable.

What is the nature of the instability which is predicted to occur when conditions (40) are satisfied? We investigate this next.

BIFURCATION TO PERIODIC STEADY STATE

The mathematical structure of the problem may be summarized as follows: Eqs.(17)-(19) representing the behavior of the system in the neighborhood of the equilibrium steady state (11)-(13), possess solutions of the form (21)-(23), which behave like $\exp(rt)$, where r is given by the cubic (30). For each n in (28), there are 3 roots to (30), all of which have negative real parts when $k < K$. As k is increased through K, a pair of roots r cross the imaginary axis in the complex plane.

If we had a sufficiently smooth vector field (C^k, $k > 3$) we could (under mild conditions that are generic) expect a Hopf bifurcation (Marsden & McCracken [10]). This would involve the birth of a periodic motion called a limit cycle in a center manifold which is tangent to the eigenspace defined by the two modes (28),(24),(25) corresponding to the pair of pure imaginary roots r. The amplitude of the limit cycle would gradually increase from zero at the bifurcation.

The present model, however, is C^0 (piecewise linear, in fact), and hence the Hopf bifurcation theorem does not apply. Nevertheless our system does exhibit a

bifurcation to a periodic motion as k goes through K. In physical terms we may think of the periodic motion as resulting from a balance between the unbounded growth which occurs in the open-pore region and the stable decay which occurs in the closed-pore region. Thus we see that the periodic motion cannot lie entirely in either region. For a given station x, the pore may be sometimes open and sometimes closed, or it may be always open, or always closed. All we can say at this point is that all the pores cannot be always open or always closed.

We may picture this by drawing in the x-t plane a curve which separates open-pore regions from closed-pore regions. Since the motion is periodic in time, we may restrict our attention to $0 < x < 1$ and $0 < t < T$, where T is the (unknown) period. See Fig. 8.

How does the bifurcation occur? Unlike the Hopf bifurcation in which the bifurcating limit cycle is born with zero amplitude, in this system the bifurcating limit cycle is born with finite amplitude. We see this as follows: At $k = K$, each station x has a u-v phase plane which is filled with closed orbits. Here we only consider the pair of pure imaginary roots $r = \pm is$, cf. eqs.(31), (32), and omit contributions associated with roots r having negative real parts (as these will decay to zero.) Each such closed orbit will be centered at the equilibrium steady state (11)-(16). Since all such equilibrium points in the u-v plane lie in the open-pore region, each located a finite distance from the closed-pore region, and since at least one station x must involve a motion of which at least one point passes through the closed-pore region, we see

that the bifurcating limit cycle must first occur with a finite amplitude. In what follows, we compute the amplitude of the limit cycle at bifurcation.

At bifurcation, the shaded region in Fig. 8 which represents those points which lie in the closed-pore region, will consist of a single point. Since each closed orbit in the u-v plane has an amplitude which varies with x like $\sin(\pi x/2)$ (from eqs.(21)-(25), (28)), the amplitude is largest when x=1. Moreover the center of the closed orbit lies along the line u+v = 2, at a distance of $2^{1/2} z_{ss}(x)$ from the closed-pore region, see Fig. 9. But the function $z_{ss}(x)$ is smallest at x=1 (from eq.(11)). Thus the station x=1 corresponds to the closed orbit which has center closest to the closed-pore region, and which has largest amplitude. Thus at the bifurcation, a closed orbit centered at x=1 just touches the line u=v (the boundary of the closed-pore region). This condition will permit us to derive an expression for the amplitude of the bifurcating limit cycle.

At $k = K$, eqs.(5),(10) exhibit solutions of the form:

$$z = z_{ss} + A \cos(s\,t) \sin(\pi x/2) \tag{41}$$

$$u = 1 + z_{ss} + A\,(B_1 \cos(s\,t) + B_2 \sin(s\,t)) \sin(\pi x/2) \tag{42}$$

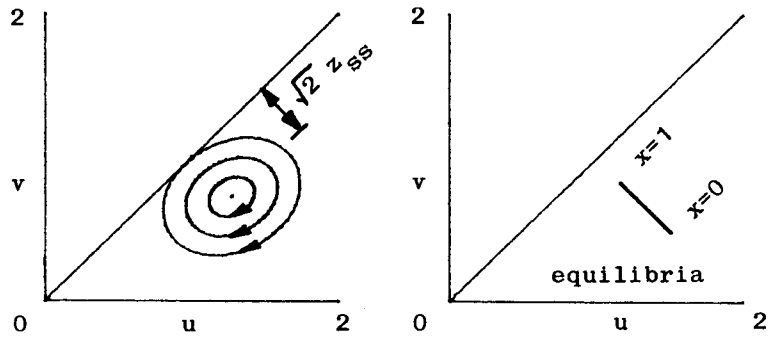

Fig. 9. At bifurcation, the u-v phase plane for a fixed station x is filled with closed orbits in the neighborhood of the steady state equilibrium point. For x varying from 0 to 1, the equilibria all lie along the line u+v = 2.

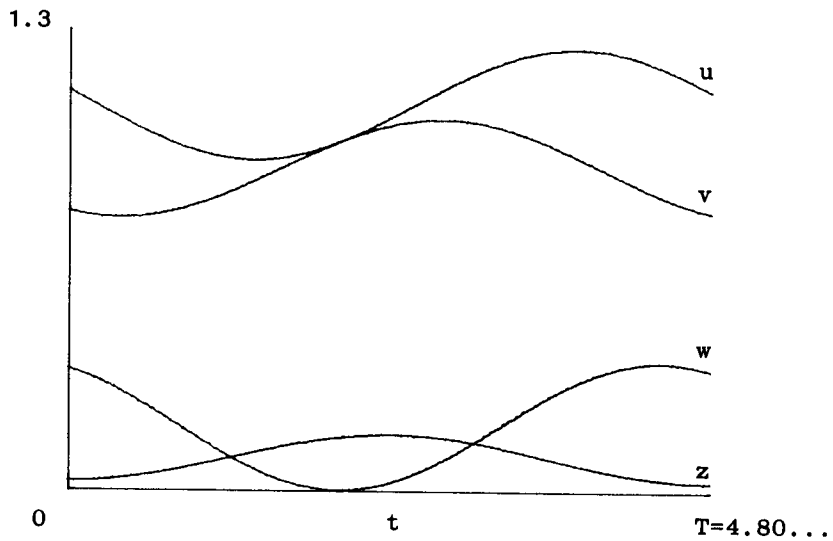

Fig. 10. Exact periodic solution at bifurcation for m=0.1, D=1, z0=0.2 at x=1. Plot of eqs.(41)-(43) with parameters as in (50)-(52).

$$(43) \quad v = 1 - z_{ss}$$

$$+ A\,(C_1 \cos(s\,t) + C_2 \sin(s\,t))\ \sin(\pi x/2)$$

where z_{ss} is as in (11), $s = b^{1/2}$ is as in (32),(30), and where the real constants B_i and C_i are obtainable from (24),(25) with r = is when these equations are respectively written in the form

$$(44) \qquad g(x) = f(x)\,(B_1 - i\,B_2)$$

$$(45) \qquad h(x) = f(x)\,(C_1 - i\,C_2)$$

For fixed values of m and D, eqs.(41)-(43) represent a 1-parameter family of solutions with the amplitude A as parameter. To find the value of A which corresponds to the bifurcating limit cycle, we set x=1 and require the motion in the u-v plane to be tangent to the line u=v:

$$(46) \qquad \frac{du}{dv} = \frac{u_t}{v_t} = 1 \quad \text{when} \quad u = v$$

From (46),(42),(43) we obtain 2 equations for the amplitude A and the time of tangential contact t* :

$$(47)\quad -B_1 \sin(s\,t^*) + B_2 \cos(s\,t^*) =$$

$$-C_1 \sin(s\,t^*) + C_2 \cos(s\,t^*)$$

$$(48)\quad z_{ss} + A\,(B_1 \cos(s\,t^*) + B_2 \sin(s\,t^*)) =$$

$$- z_{ss} + A\,(C_1 \cos(s\,t^*) + C_2 \sin(s\,t^*))$$

Solving (47) for t* and substituting in (48), we obtain

$$(49)\quad A = -\frac{2\,z0}{\cosh p}\,[(B_1 - C_1)^2 + (B_2 - C_2)^2]^{-1/2}$$

where $p = (2\,K/D)^{1/2}$.

As an example, suppose we choose m = 0.1 and D = 1. Then we find from (34) that

(50) $K = 1.02138$

and from (32),(30), the frequency

(51) $s = 1.30681$

while comparison of eqs.(44),(45) with (24),(25) gives $B_1 = -0.592656$, $B_2 = 2.28215$, $C_1 = 1.82308$, $C_2 = 1.00270$

and finally (49) gives the amplitude

(52) $A = -0.331421\ z0$

Fig. 10 shows the resulting functions z,u,v,w for z0 = 0.2 at x = 1.

FINITE DIFFERENCES

In order to check the foregoing results, a finite difference scheme was used to numerically integrate eqs.(5),(10) with the boundary conditions (8),(9). Ten pivotal points were chosen in the x-direction involving a step size of 0.1, with a time step of 0.001. The numerical error associated with the finite difference scheme then turned out to be of the order of 0.1.

The behavior displayed in Fig. 10 was corroborated to within the size of the numerical errors.

In addition, the computer program was used to follow the bifurcating periodic motion beyond the point of bifurcation. Fig. 11 shows the numerically obtained curve separating open-pore states from closed-pore states in the x-t plane, as a function of k for m=0.1 and D=1 (cf. Fig. 8.) Fig. 12 plots the fractional area in the x-t plane occupied by the closed-pore region in Fig. 11, as a function of k, and exhibits the familiar pitchfork bifurcation. (The numerically obtained bifurcation value of K=1.26 differs due to numerical error from the exact value of K=1.02, cf. eq.(50).)

The finite difference scheme was also used to investigate the transient response of the model in a parameter range for which the equilibrium steady state was stable. We initialized the leaf in steady state equilibrium at $z(x,t)=-0.2$ (closed-pore), $u(x,t)=0.8$, $v(x,t)=1.2$, and at $t=0$ suddenly applied an increase in water potential to the petiole, $z(0,t)=0.2$. According to the previous analysis, for $m=0.1$ and $D=1$, this will lead to an equilibrium steady state of the form of eqs.(11)-(13) for which all pores are open.

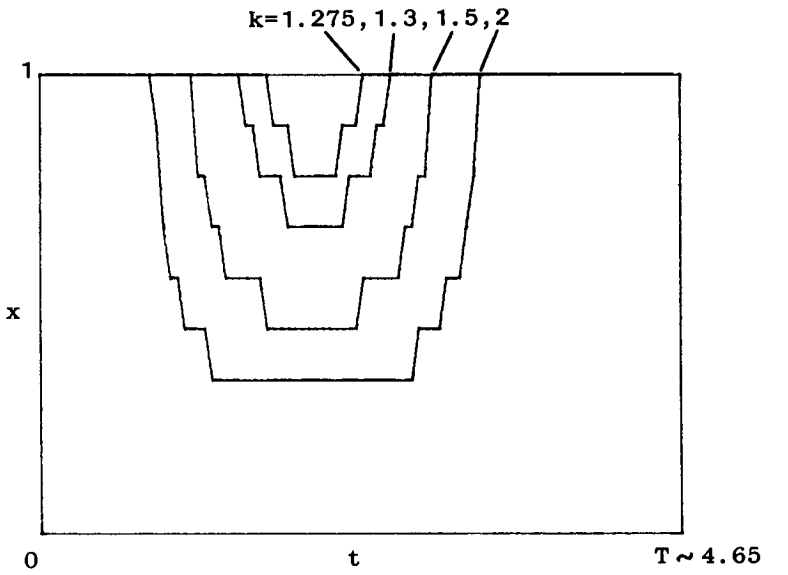

Fig. 11. Numerically obtained curves separating open-pore states from closed-pore states for m=0.1, D=1 and various k. Cf. Fig. 8.

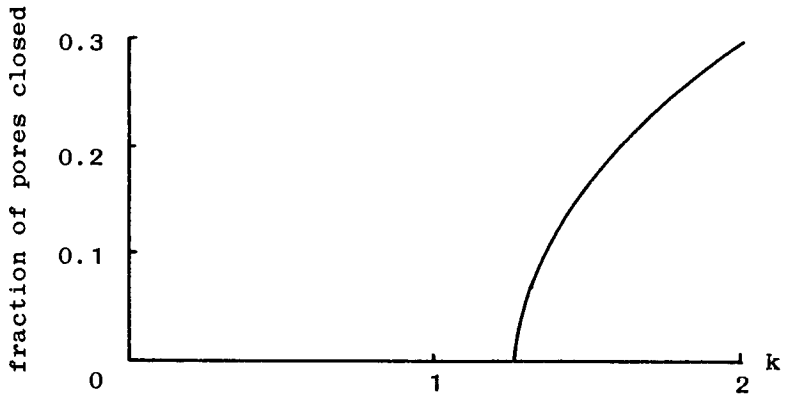

Fig. 12. Fractional area in the x-t plane of Fig. 11 occupied by closed pore region, as a function of k.

The numerical results for m=0.1 and D=1 are displayed in Fig. 13 for k=0.5, 1, respectively. Note that there may occur several waves of closing before the leaf finally stays open. This qualitative behavior of the model is in agreement with experimental observations based on the previously discussed video recordings of the leaf surface.

SUMMARY AND CONCLUSIONS

The model presented in this paper represents a distillation of numerous previous works which model the stomatal dynamics of leaves. The main ingredient of the model consists of a piecewise continuous flow on the phase plane (physically reflecting the distinct dynamics occurring when the individual stomate is open or closed, cf. Fig. 3), coupled over the leaf surface by the diffusion of water potential. In the nonspecific form given by eqs.(2),(3) and (6), this model offers a general approach to leaf dynamics. In this paper, however, we considered a special case in which the flow on the u-v pressure plane was taken to be linear (eq.(5)), and in which the leaf efflux due to evaporation Q(w) was taken to be a linear function of the pore size w (cf. eqs.(6),(7)).

We found that due to a bifurcation involving the loss of stability of the equilibrium steady state, the whole leaf model could exhibit steady state periodic behavior (even though the linear flow modeling the individual stomate could not.) A more extensive analysis of this model, including an investigation of the possibility of additional bifurcations, remains to be done.

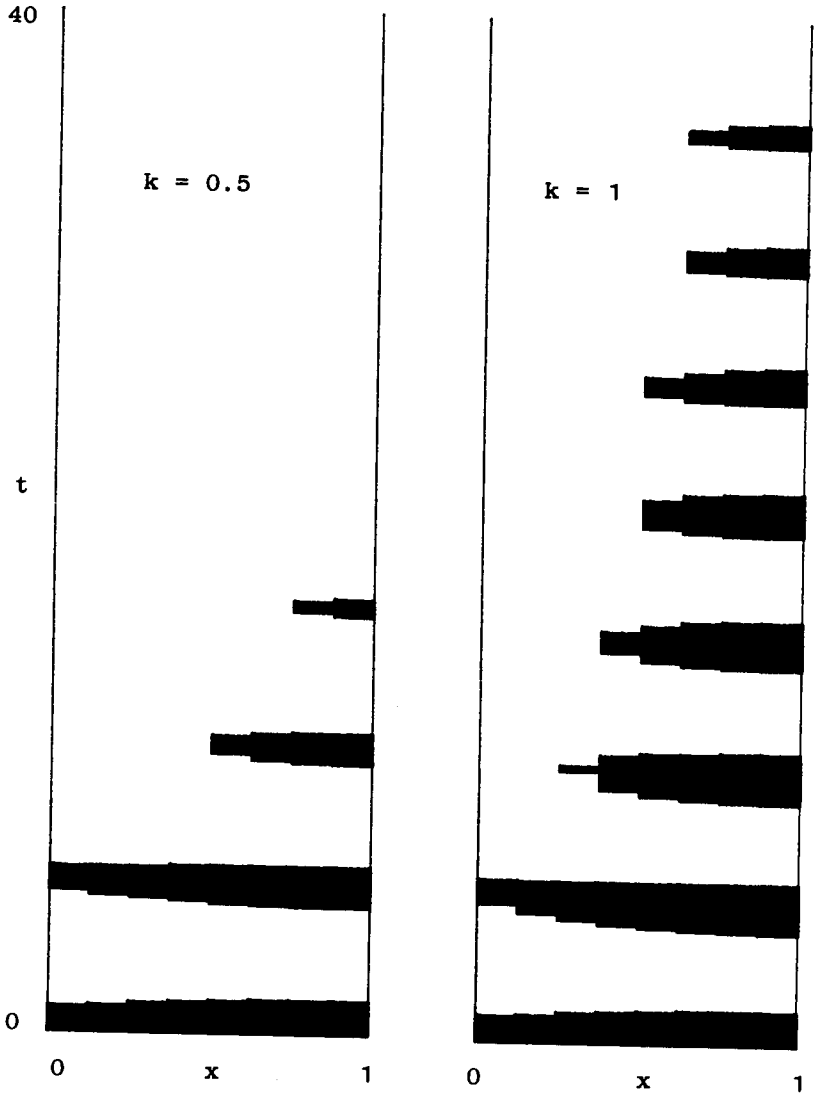

Fig. 13. Transient response obtained by numerical integration for m=0.1, D=1 and for k=0.5, 1. Shaded (unshaded) regions represent closed (open) pores.

A numerical investigation of the transient behavior of the model showed that the leaf surface may experience several waves of stomatal opening and closing before equilibrium is reached. Since each cycle may typically take 20 to 30 minutes, the transient behavior could account for several hours of leaf dynamics. Although our model took the leakage coefficient k to be a constant, it is more accurately modeled as depending upon the boundary layer thickness of the still air adjacent to the leaf, as well as upon the illumination of the leaf. Thus k could change with windspeed or with the passage of a cloud over the leaf, thus creating additional sources of transient behavior.

With the biologist in mind, we now attempt to complement the mathematical analysis presented in this paper with an explanation in words of the oscillations and waves involved in our model of leaf dynamics. The interaction in time, at a fixed leaf position, between the water potential z and the pore width w may be described as follows: When w is positive, the efflux through the open pore reduces z, which in turn eventually causes w to decrease (since the individual stomate model is assumed to depend on z.) This relationship tends to produce an oscillation in which w and z are approximately 180 degrees out of phase. This is illustrated in the exact solution of Fig. 10, as well as in our finite difference computer simulations. The wave-like spatial dependence of these oscillations may be understood by contrasting the conditions at the petiole (x=0 in the model) with those at the leaf edge (x=1 in the model). Water from the petiole has farther to travel to replenish those stomatal units near the leaf edge and thus these units

encounter a lag in water potential z relative to stomata closer to the petiole. This lowering of z causes the units near the leaf edge to close, and a wave of stomatal closing is observed to move towards the petiole (cf. Fig. 13.) Once these stomata are closed, new water from the petiole accumulates near them, and since the units closer to the petiole are replenished more effectively than those more distant, a wave of opening moves from the petiole to the leaf edge.

Our model studies were motivated by experimental observations based on delayed light emission. Video recordings of the leaf surface plainly show waves of stomatal opening moving across the leaf.

It is hoped that the experimental evidence of stomatal oscillation fields, as well as the existence of a relatively tractable model, will stimulate additional investigations in this area.

REFERENCES

1. Rand, R.H., "Fluid Mechanics of Green Plants", Annual Rev. Fluid Mechanics, 15:29-45 (1983)

2. Nobel, P.S., "Introduction to Biophysical Plant Physiology", Freeman (1974)

3. Delwiche, M.J., Cooke, J.R., "An Analytical Model of the Hydraulic Aspects of Stomatal Dynamics", J. Theoretical Biology, 69:113-141 (1977)

4. Rand, R.H., Upadhyaya, S.K., Cooke, J.R. and Storti, D.W., "Hopf Bifurcation in a Stomatal Oscillator", J. Math. Biology, 12:1-11 (1981)

5. Rand, R.H., Storti, D.W., Upadhyaya, S.K. and Cooke, J.R., "Dynamics of Coupled Stomatal Oscillators", J. Math. Biology, 15:131-149 (1982)

6. Ellenson, J.L. and Amundson, R.G., "Delayed Light Imaging for the Early Detection of Plant Stress", Science, 215:1104-1106 (1982)

7. Cooke, J.R., Debaerdemaeker, J.G., Rand, R.H. and Mang, H.A., "A Finite Element Shell Analysis of Guard Cell Deformations", Trans. Amer. Soc. Agricult. Eng., 19:1107-1121 (1976)

8. Holcomb, D.P. and Cooke, J.R., "An Electrolytic Tank Analog Determination of Stomatal Diffusion Resistance", Amer. Soc. Agricult. Eng. paper no. 77-5510, Amer. Soc. Agricult. Eng., St. Joseph, Michigan (1977)

9. Cooke, J.R. and Rand, R.H., "Diffusion Resistance Models", in "Predicting Photosynthesis for Ecosystem Models", ed. J.D. Hesketh and J.W. Jones, 1:93-121, CRC Press (1980)

10. Marsden, J.E. and McCracken, M., "The Hopf Bifurcation and its Applications", Springer Verlag (1976)

DEPARTMENT OF THEORETICAL & APPLIED MECHANICS
AND
BOYCE THOMPSON INSTITUTE FOR PLANT RESEARCH
ITHACA, NEW YORK 14853